Waste and Biomass Valorization
https://doi.org/10.1007/s12649-024-02629-7

ORIGINAL PAPER

Valorisation of Metallurgical Waste for Inorganic Pigments Production

D. C. Paz-Gómez[1,2] · I. S. Vilarinho[2] · J. Carvalheiras[2] · S. M. Pérez-Moreno[1] · Maria P. Seabra[2] · João A. Labrincha[2] · J. P. Bolívar[1]

Received: 6 October 2023 / Accepted: 17 June 2024

Abstract

Four industrial wastes, namely, tionite (T), iron grit (IG), electroplating sludge (ES), and mill scale (MS), are typically disposed of in controlled hazardous landfills because of their toxic content, posing potential harm to human health and to the environment. At the same time, the chemical composition of these wastes, specifically the nature and content of transition metals, makes them potentially attractive for reuse in pigments manufacturing. This work details the study of these residues for producing coloured perovskites to be tested as inorganic pigments. The residues were mixed, in different proportions, and subsequently calcined to produce the required structures. The colouring potential was then assessed in a ceramic paste and in a transparent glaze. Leaching tests were carried out to verify the effective immobilisation of the hazardous species. Dark pigments were successfully obtained from the mixtures of T: ES: Co_3O_4, T: MS and T: IG. The crystalline phases present in T: ES: Co_3O_4 are nickel–chromium iron oxide spinel–$Fe_{1.5}Cr_{0.5}NiO_4$ (without Co) or trevorite–Fe_2NiO_4 (with Co), titanium nickel oxide–$TiNiO_3$ and titanite–$CaTiSiO_5$. The mixtures T: MS and T: IG presented hematite (Fe_2O_3) and pseudobrookite (Fe_2TiO_5). Leaching tests confirmed the non-hazardous or inert character of the synthesized pigments. Products showed brownish or greyish hues, depending on the pigment added. T:75ES_1100, T:73ES:2Co_1100, T:75MS_1000, T:75MS_1100 and T:75IG_1000 pigments can effectively and safely be used to colour ceramic paste replacing partially or totally the commercial pigments.

Keywords Tionite · Electroplating sludge · Slag · Inorganic pigments · Residue valorisation

Introduction

Inorganic pigments are compounds known for their ability to add vibrant hues to materials without undergoing chemical or thermal reactions. Widely employed across industries such as ceramics, cosmetics, and textiles due to their stability, durability, and wide range of colours. An inorganic pigment is a transition metal bearing complex structure formed by a heat treatment process, which shows: (a) thermal stability, maintaining its identity at high temperature; (b) chemical stability, not reacting when fired with glazes or ceramic matrices; and (c) high colouring power when dispersed in the matrices [1, 2]. Inorganic pigments distinguish themselves from dyes primarily through their chemical composition, application method, and interactions with the material they colour. Unlike dyes, which typically consist of organic compounds soluble in their application medium, pigments generally remain insoluble, dispersing as solid particles within the medium. Dyes feature conjugated systems of double bonds, enabling them to absorb light and

✉ D. C. Paz-Gómez
daniela.paz@dci.uhu.es

✉ I. S. Vilarinho
inessvilarinho@ua.pt

✉ João A. Labrincha
jal@ua.pt

J. Carvalheiras
jcarvalheiras@ua.pt

S. M. Pérez-Moreno
silvia.perez@dci.uhu.es

Maria P. Seabra
pseabra@ua.pt

J. P. Bolívar
bolivar@uhu.es

[1] Department of Integrated Sciences, Research Centre on Natural Resources, Health and the Environment (RENSMA), University of Huelva, Huelva 21007, Spain

[2] Department of Materials and Ceramic Engineering/CICECO-Aveiro Institute of Materials, Campus Universitário de Santiago, University of Aveiro, Aveiro 3810-193, Portugal

Published online: 26 June 2024

manifest vibrant colours. Further, dyes may exhibit lesser durability and heightened susceptibility to fading over time, particularly when exposed to light, heat, or chemical agents, when compared to pigments [3, 4].

The attempts to use industrial waste in the production of inorganic pigments has witnessed significant growth over recent decades, propelled by the expanding ceramic material market and rising raw material expenses [5–7]. Presently, there is a notable surge in interest surrounding the recycling, reusing, and repurposing of waste materials, aligning with contemporary global trends, as it not only yields economic advantages but also fosters environmental sustainability. This trend harmonizes with the current European Union strategy for Circular Economy [8], underscoring the imperative to extract maximum value from resources while minimizing waste and environmental impact. Several industrial wastes, such as red mud [6, 9], electroplating sludge [5, 10], wiredrawing sludge [11, 12] and others [13–15], were already tested as raw materials for pigments due to their chemical composition, specifically the nature and content of transition metals [7]. Besides fulfilling the three main characteristics, the inorganic pigments prepared from industrial wastes must also immobilise the hazardous species to prevent their leaching into the environment [16].

The main environmental benefits of using industrial hazardous residues as raw materials are the immobilisation of toxic species into the glazes or ceramic matrices, as well as, decreasing the virgin raw materials consumption. Currently, tionite (T), contaminated iron grits (IG), electroplating sludge (ES) and mill scale (MS) have no commercial value and are mostly disposed of in landfills for hazardous waste, except for the MS. This management strategy involves high transportation and storage costs which raises environmental concerns [10, 12, 17].

In the literature, there have been some studies about the use of tionite as secondary raw material in ceramic bodies and bricks [17, 18]. In the case of iron-rich wastes, such as mill scales, steel residues or untreated iron ore gangue, there are some authors reporting their use in ceramic products [19], in the preparation of ceramic colorants [15] and pigments [13, 20]. Regarding pigments, Legodi et al. [20], prepared iron oxide pigments using specific precursors from mill scale iron waste. Magnetite and goethite were precipitated from their respective precursors in aqueous media. Distinct red shades of hematite were obtained by the calcination of the precipitated goethite at temperatures ranging from 600 to 900 °C. Maghemite was obtained by thermal treatment of magnetite at 200 °C. The authors suggest that the prepared pigments can show high tinting strength, quality hiding power and good oil absorption. However no further tests were conducted. Prim et al. [13] used iron oxide from a metal sheet rolling process as chromophore. Different amounts of hematite and silica were homogenized by milling and then the powders were calcined between 1050 and 1200 °C. The pigments were applied in a porcelain body, developing a pink hue, and in a ceramic enamel but in this case no colour was developed. The authors suggest that this could be a result of the presence of zinc in the composition of ceramic glaze, but the detection of crystalline phases was not performed.

ES has been reported as a precursor for the production of inorganic pigments or to directly colouring ceramic bodies, bricks and other decorative ceramic products [6, 10, 21]. Carneiro et al. [5]. studied the combination of ES with red mud in different proportions, being the mixtures calcined at 1200ºC. Black and brown pigments were obtained but incorporation tests in ceramic products were not conducted and the immobilization of the hazardous species was not evaluated.

The novelty of the present paper is the attempt to recycle four hazardous wastes - tionite (T), iron grit (IG), electroplating sludge (ES), and mill scale (MS) in the production of inorganic pigments. These residues were blended in different proportions and subjected to calcination at two temperatures (1000 and 1100ºC) to generate stable pigmenting structures. Their colouring power was tested in a ceramic product and in a transparent glaze. Ultimately, leaching tests were carried out to confirm the immobilisation of the hazardous species, assuring their safe use.

Materials and methods

Materials

The wastes used as raw materials come from different industries. A titanium dioxide producer in Huelva, Spain, provided the undissolved ilmenite sludge, called tionite (T). Contaminated IG was supplied by the CEPSA refinery in Huelva, Spain. ES was provided by Grohe, Portugal, a Cr-Ni electroplating industry. MS was given by Fapricela - Indústria de Trefilagem S.A., Portugal, and is generated from steel wiredrawing production. The cobalt (III) oxide (Co_3O_4) employed in this work was of analytical grade (purity > 99.8 wt %) with particle size < 50 nm, from Aldrich Chemistry. All materials were received in the form of powders that before its use were dried and milled.

The transparent powdered glaze was supplied by Esmalglass-Itaca Group, while the stoneware ceramic paste tested belongs to Grestel - Produtos Cerâmicos S.A. Moreover, a commercial deflocculant (Dolapix) was used to adjust the viscosity of the slurry.

Pigments Preparation

The compositions prepared in this study are outlined in Table 1, aiming to reach black hues. Cobalt was incorporated (2 and 5 wt% Co_3O_4) in the formulations, to accentuate the darkness. The amount of tionite was kept constant (T = 25 wt%), so the designation of each pigment attempts to be intuitive: e.g. T:73ES:2Co_1000 corresponds to a mixture of 25 wt% T + 73 wt% ES + 2 wt% Co_3O_4, fired at 1000 °C.

The raw materials were subjected to wet ball milling (with water) at 200 rpm for 12 h to ensure a good homogenization. Subsequently, the mixtures underwent drying at 80ºC, followed by firing in an electric furnace under a static airflow. The heating and cooling processes occurred gradually at a rate of 5 ºC/min until reaching maximum temperatures of 1000 ºC and 1100 ºC, as indicated in Table 1. The materials were held at these temperatures for 2 h to ensure proper synthesis. Finally, the resulting pigments were disaggregated and sieved at 63 µm.

Test in Glaze and Ceramic Paste

The tinting power of the prepared pigments was tested in a transparent glaze and in a stoneware ceramic paste. In the case of the glaze, 3 wt% of each pigment was added, and the homogenisation process was conducted by wet mixing in a ball mill for 60 min at 200 rpm. The slurry was then dried at 80 °C and the obtained powder was disaggregated and sieved (63 µm). Subsequently, the powders were pressed into 25 mm pellets and fired in an electric furnace under static airflow, with a heating and cooling rate of 10 ºC/min until the maximum temperature of 1100 ºC (30 min dwell time).

In the ceramic paste, suspensions with 3 and 5 wt% of pigments were prepared. The homogenisation of the suspensions was conducted by manually mixing for 2 min. Then, the mixture was sieved at 425 µm and dried in a gypsum plate until it reached the desired humidity (≈ 20 wt%). The pastes were stored, at room temperature, in closed plastic bags to avoid drying until the preparation of the specimens, similar to what was done in [22]. Afterwards, specimens (30 × 20 × 10 mm) were obtained by plastic pressing in a uniaxial hydraulic press. Then, 15 mm marks were placed on each specimen to evaluate the shrinkage after drying at 120 ºC for 24 h. Finally, the samples were fired in a laboratory muffle. The firing cycle simulates the one used in the industry for this type of (stoneware) product: (i) heating rate of 3 ºC/min until 575 ºC and 30 min of dwell time; (ii) heating rate of 5 ºC/min until 770 ºC and 60 min of dwell time; (iii) heating rate of 5 ºC/min until 1220 ºC and 30 min of dwell time; and (iv) cooling until ambient temperature as in article [19].

The specimens were codified as "X/Y," where "X" is the code of the pigment, and "Y" represents the testing substrate: glaze (G) or ceramic paste (P). The numbers express the added amount of pigment. For example, the code T:75ES_1000/G3 corresponds to the use of the T:75ES_1000 pigment (3 wt%) in the transparent glaze (G).

Table 1 Compositions, designations and firing temperature of the prepared pigments

Code pigment	Compositions (wt%)	Max. Processing Temperature (ºC)
	T: ES: Co_3O_4	
T:75ES_1000	25:75:0	1000
T:75ES_1100		1100
T:73ES:2Co_1000	25:73:2	1000
T:73ES:2Co_1100		1100
T:70ES:5Co_1000	25:70:5	1000
T:70ES:5Co_1100		1100
	T: MS	
T:75MS_1000	25:75	1000
T:75MS_1100		1100
	T: IG	
T:75IG_1000	25:75	1000
T:75IG_1100		1100

Characterization Techniques

Raw Material Characterisation

The chemical composition of the wastes was assessed by X-ray fluorescence (XRF) employing a Philips X'Pert PRO MPD spectrometer, and the loss on ignition (LOI) at 1000 °C was also determined. The particle size distribution was obtained by laser dispersion in a HORIBA Scientific analyser, model LA-960V2. Furthermore, the mineralogical composition, at room temperature, was evaluated through X-ray diffraction (XRD) analysis using a Panalytical X'Pert PRO diffractometer equipped with Ni filtered Cu X-ray source and PIXcel^{1D} detector, operating under the following conditions: voltage 45 kV; current, 40 mA; range 20–60° 2Θ; step size 0.026°, time per step 2s.

Pigments, Glaze, and Ceramic Pastes Characterisation

The mineralogical composition of the obtained pigments was also analysed by XRD. Moreover, the optical properties were measured by diffuse reflectance spectroscopy using a Shimadzu UV–3100 UV–Vis–IR spectrometer in the UV-vis range 190–950 nm. Reflectance (R) was converted to absorbance (Kubelka–Munk) by the equation: Absorbance Kubelka-Munk = $(1R)^2/2R$ [23, 24]. L*a*b* colour coordinates were measured with a Konica Minolta Chroma Meter. The CIEL*a*b* data are expressed as brightness L*,

changing from 0 (black) to 100 (white), a* (+red, -green), and b* (+yellow, -blue) [25, 26].

On the other hand, the colour evaluation of the prepared specimens (glazes and pastes) was also done based on the three-dimensional CIEL*a*b* projection. The linear firing shrinkage was evaluated by measuring the length of the specimen before and after firing. The weight loss (%) upon firing was also determined.

Leaching Experiments

Leaching tests were carried out to evaluate the mobility of the hazardous species from the pigment. The adopted procedure followed the EN 12457-2 protocol [27]. So, distilled water was used as extraction fluid, at a liquid/solid ratio of 10 L/kg (±2 wt%) and during 24 ± 0.5 h. Then, the solution was collected, and the concentration of the hazardous species was measured in a total reflection X-ray fluorescence spectrometer (TXRF—S2 PICOFOX 50 keV), with a detection limit of ppb.

Other set of leaching tests was performed according to the EU Ceramic Directive 84/500/ECC [28], aiming to assure the safe of ceramic tableware products, in which a 4 vol% acetic acid solution (CH_3COOH) was used as the extraction fluid. This solution was prepared using a glacial acetic acid and distilled water. Initially, the specimens were washed with detergent and rinsed with tap water, followed by distilled water. After these, the samples were dried and submerged in the acetic acid solution for 24 h at room temperature. Finally, the solutions were also analysed by TXRF.

Table 2 Chemical composition of the wastes (assessed by XRF), and main crystalline phases detected by XRD

	Residues			
	T	IG	ES	MS
Component	(wt%)			
Al_2O_3	2.90	2.60	1.70	0.10
CaO	0.66	1.30	1.10	0.07
Fe_2O_3	10.0	64.0	0.65	98.0
K_2O	0.47	0.64	0.07	-
MgO	0.73	0.76	0.16	0.07
MnO	0.39	0.04	-	0.40
Na_2O	0.61	0.64	-	-
SiO_2	17.0	24.0	5.60	0.46
SO_3	10.0	1.00	5.80	-
P_2O_5	0.03	0.11	4.50	-
TiO_2	44.0	0.31	0.03	-
Cr*	0.32	0.04	15.0	0.07
Cu*	0.03	1.60	2.20	1.10
Ni*	0.01	0.03	26.0	-
Pb*	0.04	0.46	0.90	-
Zn*	0.02	1.50	1.60	-
LOI	12.0	0.03	34.0	0.01
Main crystalline phases				
Rutile (TiO_2)	X	-	-	-
Pseudobrookite (Ti_2FeO_5)	X	-	-	-
Quartz (SiO_2)	X	-	x	-
Fayalite (Fe_2SiO_4)	-	x	-	-
Magnetite (Fe_3O_4)	X	x	-	x
Wüstite (FeO)	-	-	-	x
Eskolaite (Cr_2O_3)	-	-	x	-
Bunsenite (NiO)	-	-	x	-

*total

Results and Discussion

Wastes Characterisation

The chemical composition, loss on ignition (LOI) and the main crystalline phases of the residues are shown in Table 2. The main components of T are titanium (44 wt% TiO_2), silicon (17 wt% SiO_2), iron (10 wt% Fe_2O_3), sulphur (10 wt% SO_3) and aluminium (2.9 wt% Al_2O_3). Other elements, such as Ca, K, Mg, Mn, Cr, Cu, Na, Ni, P, Pb and Zn, were found in concentrations below 1 wt%. Titanium is mainly present as rutile (TiO_2), but part of it is associated with Fe, forming pseudobrookite (Ti_2FeO_5). Magnetite (Fe_3O_4) is also present, and a small proportion of quartz (SiO_2) was also detected. These results agreed with the chemical composition obtained by XRF and are similar to those reported in other studies [17, 18].

Iron (64 wt% Fe_2O_3) and silicon (24 wt% SiO_2) are the main components of IG, whereas aluminium, calcium, copper, and zinc were found in proportion between 1 and 5 wt%. Other elements such as Cr, K, Mg, Mn, Na, Ni, P, Pb and Ti are also present but in concentrations below 1 wt%. The XRD analysis showed that Fe was mainly associated with Si, forming fayalite (Fe_2SiO_4). However, a small Fe fraction was also found as magnetite (Fe_3O_4). Therefore, XRD results agreed with the chemical composition determined by XRF and are similar to those obtained by other authors [29–31].

The ES and MS wastes employed in this work have already been characterised in other works conducted by some of the actual co-authors [5, 10, 12, 32]. The chemical composition of the batches used in this work are shown in Table 2. ES is mainly composed of Ni and Cr (26 wt% and 15 wt%, respectively), while sulphur, silicon, phosphorus, copper, calcium, and zinc are present in concentrations below 10 wt%. Additionally, Fe, K, Mg, Ti and Pb, were found in concentrations lower than 1 wt%. The main crystalline phases detected are bunsenite (NiO) and eskolaite (Cr_2O_3). The MS residue is mainly composed of iron (98% Fe_2O_3) and the two crystalline phases detected were wüstite (FeO) and magnetite (Fe_3O_4). The loss on ignition is very low for IG and MS wastes, revealing absence of chemical

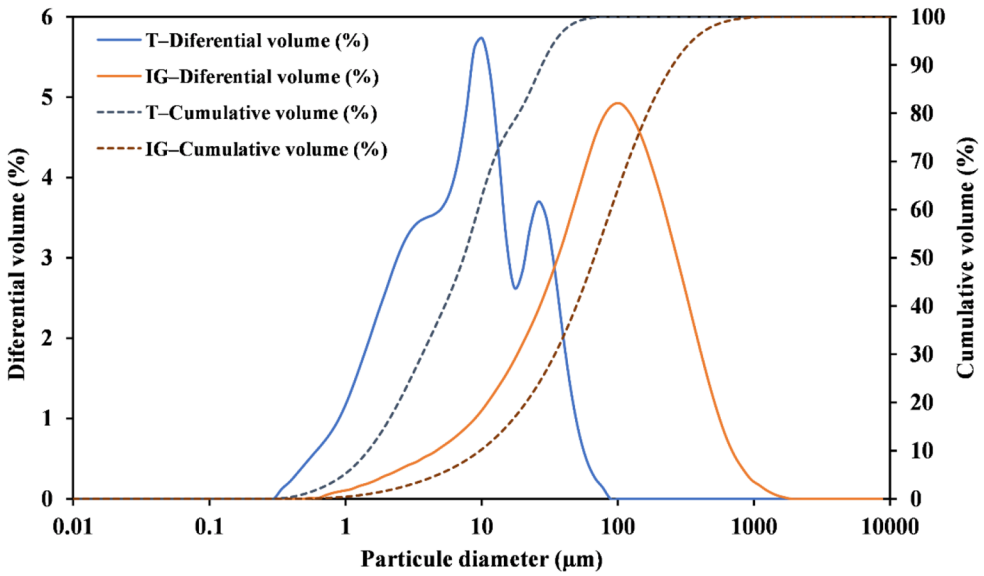

Fig. 1 Particle size distribution of T and IG samples

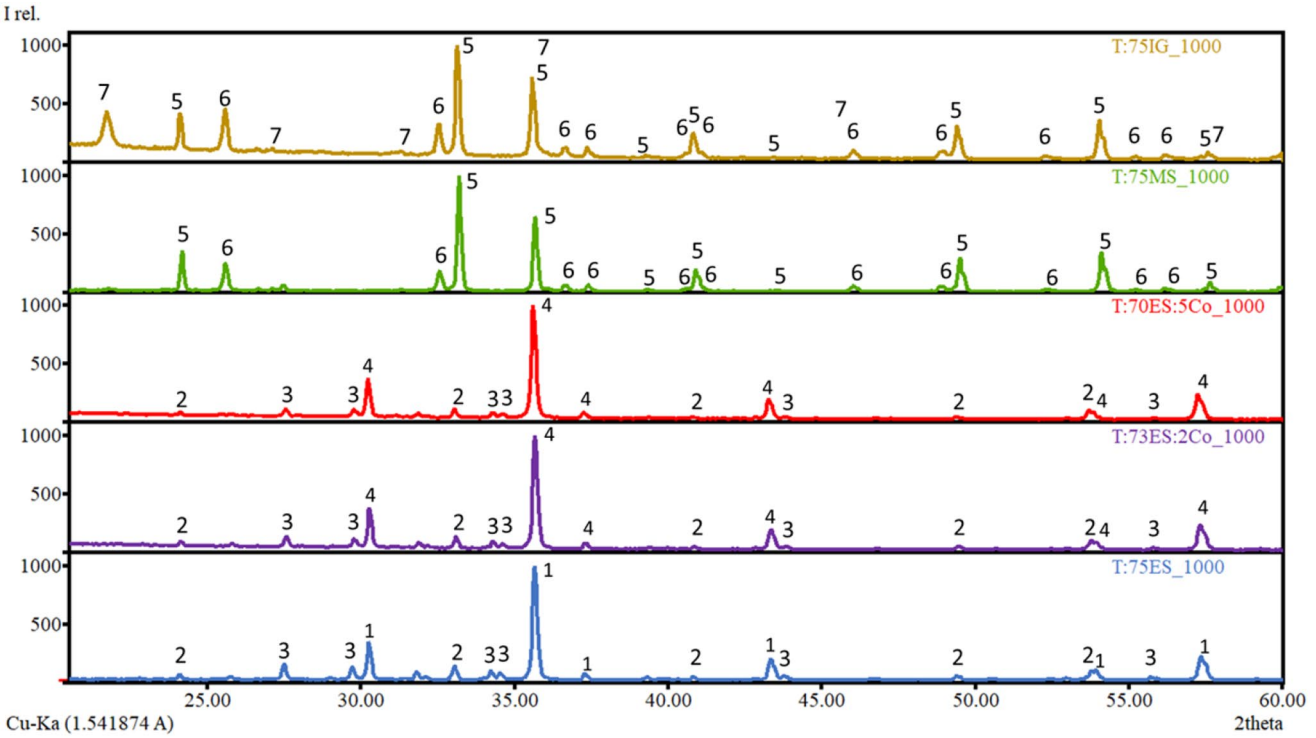

Fig. 2 XRD patterns of the pigments obtained at 1000ºC. Main crystalline phases identified: Nickel chromium iron oxide (spinel)-Fe1.5Cr0.5 NiO4 (1), titanium nickel oxide (ilmenite group)-TiNiO3 (2), titanite-CaTiSiO5 (3), trevorite-Fe2NiO4 (4), hematite-Fe2O3 (5), pseudobrookite-Fe2TiO5 (6) and quartz-SiO2 (7)

decomposition upon heating. By contrast, ES shows a high LOI, due to the presence of hydroxides and sulphates in the sludge. Tionite also suffers chemical decomposition upon firing, but less expressive than ES.

The particle size distribution plays a crucial role to control the mixing procedure and define the calcination temperature of the pigments, as it directly impacts the reactivity. It also affects the colour development and the hue intensity [33]. The particle size distribution of T and IG wastes is shown in Fig. 2. The granulometric analysis was carried out after milling in a ring miller (Retsch, RS 100, Haan, Germany). Tionite presented a median particle size (D_{50}) of 7.34 µm, indicating relatively high fineness. Conversely, iron grits show a significantly higher D_{50} of around 88.5 µm. Furthermore, previous studies [5, 10, 32] have reported that ES particles have an average particles size of about 112 µm,

with a wide particle size distribution ranging from submicro sizes to grains of around 500 µm (D_{90} = 337.9 µm) due to the presence of agglomerates. MS, on the other hand, initially presented a D_{50} of 250 µm, being then reduced to around 50 µm through milling. Moreover, approximately 98 wt% of the particles were smaller than 200 µm [12]

Pigments Characterisation

The X-ray diffraction (XRD) patterns for the mixtures fired at 1000 ºC are shown in Fig. 2. The crystalline phases present in the T:75ES_1000 mixture are a nickel-chromium iron oxide spinel ($Fe_{1.5}Cr_{0.5}NiO_4$), titanium nickel oxide ($TiNiO_3$) belonging to ilmenite group (sharing the same crystalline structure of ilmenite), and titanite ($CaTiSiO_5$). Upon adding cobalt (T:73ES:2Co_1000 and T:70ES:5Co_1000), a different spinel named trevorite (Fe_2NiO_4) was formed alongside the presence of titanium nickel oxide and titanite. The thermal transformation of Fe_2TiO_5 and Fe_3O_4 [34], present in the T residue, led to the formation of the spinel compound. The formation of $TiNiO_3$ results from the reaction between TiO_2 and NiO present in the ES waste. [35, 36]. The availability of calcium, silicon and titanium is required for the formation of titanite [37].

On the other hand, when tionite was mixed with iron-rich residues (T:75MS_1000 and T:75IG_1000), the resulting pigments presented hematite (Fe_2O_3) and pseudobrookite (Fe_2TiO_5). The formation of hematite is expected at high temperatures from the oxidation of magnetite and wüstite [38, 39]. In addition, quartz was detected in the mixture T:75IG_1000, due to the thermal decomposition of the fayalite present in IG [40, 41] or, more probably, as unreacted quartz present in T. The pseudobrookite detected in these pigments comes from the T residue, from the thermal transformation of rutile in the presence of Fe_2O_3 [42]. It should be noted that the same crystalline phases were identified in the mixtures fired at 1100 ºC.

The optical properties of the pigments calcined at 1000 ºC and 1100 ºC are shown in Fig. 3. Formulations obtained from the mixtures of T and ES are dominated by Ni^{2+} and Cr^{3+} optical signatures (Fig. 3a). Ni displays two distinct absorbance bands. The lower energy band (~13,000 cm^{-1}) can be assigned to Ni (II): $^3A_{2g}$ (^3F) → $^3T_{1g}$(^3F) transitions, while a weaker band, around 19,000 cm^{-1}, corresponds to Ni (II): $^3A_{2g}$(^3F) → $^1T_{2g}$(^1D) transitions [5, 43]. Cr presents two bands at ~14,500 cm^{-1} and 22,000 cm^{-1}, which can be related to Cr (III): $^4A_{2g}$(^4F) → $^4T_{2g}$(^4F) and Cr (III): $^4A_{2g}$(^4F) → $^4T_{1g}$(^4F) transitions, respectively [43–45]. According to previous studies [9, 44], the lower energy absorbance bands (i.e., 13,000–14,500 cm^{-1}) of Ni^{2+} and Cr^{3+} are responsible for blue/green colouration, whilst the higher energy absorbance bands (i.e., 19,000–22,000 cm^{-1}) contribute to red/orange colouration.

The pigments obtained from mixtures of T: MS and T: IG are dominated by Fe^{3+} optical signatures (Fig. 3b). Fe exhibits two appreciable absorbance bands at ~18,000 cm^{-1} and 25,000 cm^{-1}, that are due to Fe (III): $^6A_1$(^6S) → ^4E,^4A(^4G) and Fe (III) $^6A_1$(^6S) → ^4E,^2T(^4D) transitions, respectively [5, 43, 46]. According to the literature [9], these absorption bands are responsible for the observed red/orange/yellow hues. In all cases, the optical spectrum of these pigments reveals large energy signals (> 27,000 cm^{-1}) that can be attributed to charge transfers between metals and oxygen [43].

The CIELab colour coordinates of the pigments are presented in Table 3. In general, it is observed that as the firing temperature increases from 1000 ºC to 1100 ºC, the lightness (L*) as well as the red (a*) and yellow (b*) hues decrease, which is in agreement with other studies [9, 47]. In the case of the T: ES: Co_3O_4 mixture, the addition of cobalt did not cause significant changes in the lightness, which ranged between 26 and 29, for T: ES: Co_3O_4 fired at 1000 ºC, and 35–39 for T: ES: Co_3O_4 fired at 1100 ºC. However, the pigment T:72ES:3Co_1100 showed a noticeable increase in lightness, likely due to a combined effect of increased cobalt content and firing temperature. However, cobalt addition led to a slight decrease in red hue, from 0.96 to -0.05 for pigments T:75ES_1000, T:73ES:2Co_1000 and T:73ES:5Co_1000 and from 0.84 to -0.52 for pigments T:75ES_1100; T:73ES:2Co_1100 and T:73ES:5Co_1100. Conversely, the yellow-blue component exhibited significant changes with cobalt addition. The values shifted from 2.45 (for T:75ES_1000) to -0.28 and −0.48 (for T:73ES:2Co_1000 and T:70ES:5Co_1000, respectively) and from values 2.13 (for T:75ES_1100) to -1.36 and −1.23 (for T:73ES:2Co_1100 and T:70ES:5Co_1100, respectively), indicating an increase of the blue hue. It is worth noting that increasing the Co amount in the pigment fired at 1000 ºC intensifies the blue hue. Therefore, the cobalt addition leads to a decrease in the a* and b* colour coordinates, in agreement with previous studies [11, 16].

The T: MS and T: IG mixtures exhibited noticeably higher lightness compared to the T: ES: Co_3O_4 mixtures, with the exception of the pigment T:70ES:5Co_1100, which displayed a similar value to that obtained for these mixtures at 1100 ºC (colour coordinate L*~ 45–47). Furthermore, the red and yellow hues were significantly intensified, resulting in distinctive brownish tone hue attributed to the formation of pseudobrookite. Previous studies have highlighted pseudobrookite´s structural characteristics as the key factor responsible for this specific hue [9, 46].

The results of the pigments leaching are presented in Table 4. To assess their inertness, the data were compared to

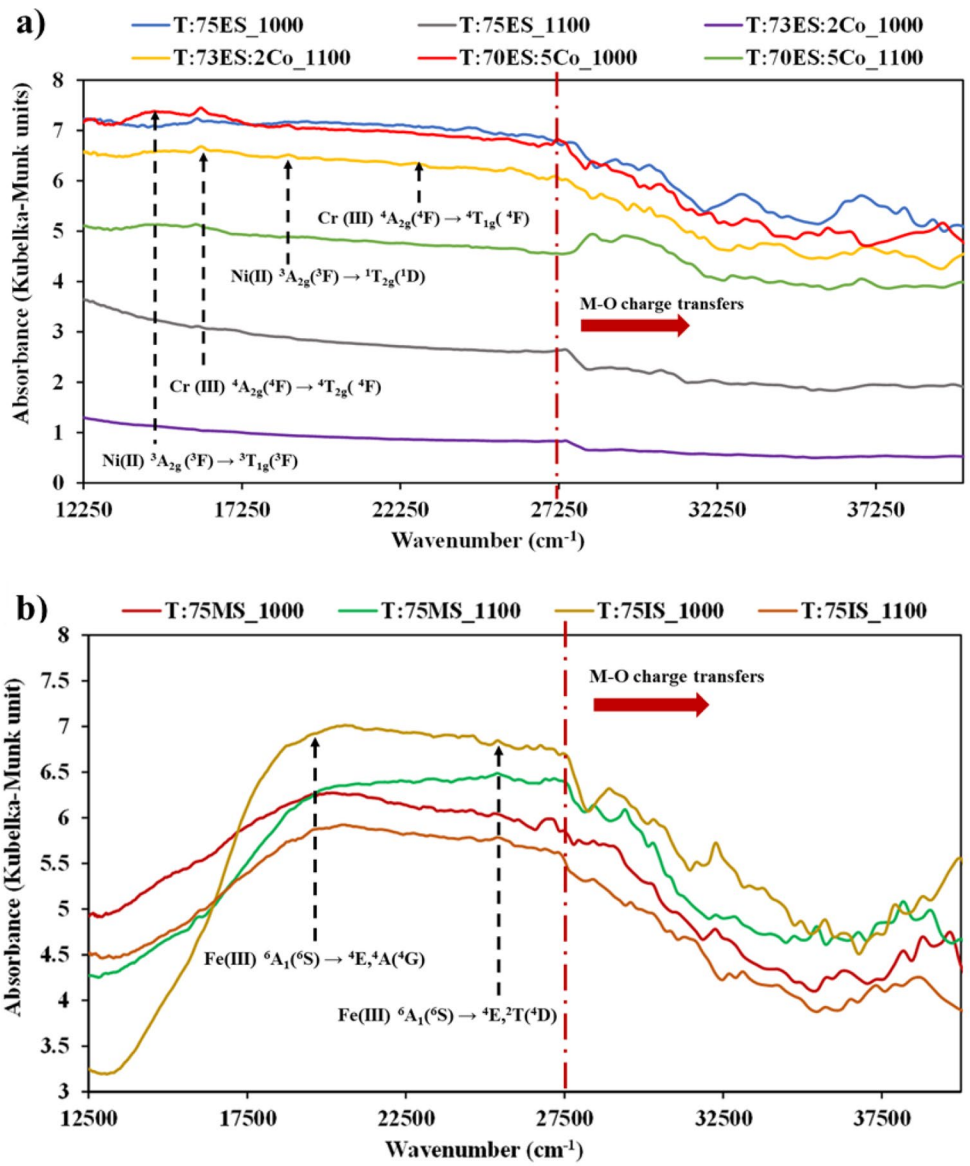

Fig. 3 Optical spectrum of the pigments fired at 1000 ºC and 1100 ºC. (**a**) T: ES: Co mixtures. (**b**) T: MS and T: IG mixtures

Table 3 CIEL*a*b colour coordinates of the obtained pigments

Pigment ID	L* 0 (Black) to 100 (White)	a* (+Red, - Green)	b* (+Yellow, -Blue)
T:75ES_1000	26.28 ± 0.63	0.96 ± 0.11	2.45 ± 0.15
T:75ES_1100	35.57 ± 0.16	0.84 ± 0.01	2.13 ± 0.02
T:73ES:2Co_1000	28.35 ± 0.06	-0.04 ± 0.02	-0.28 ± 0.02
T:73ES:2Co_1100	45.99 ± 0.14	-0.52 ± 0.01	-1.36 ± 0.01
T:70ES:5Co_1000	28.97 ± 0.05	-0.05 ± 0.02	-0.48 ± 0.01
T:70ES:5Co_1100	38.62 ± 0.59	-0.55 ± 0.03	-1.23 ± 0.04
T:75MS_1000	38.53 ± 0.09	2.15 ± 0.05	2.08 ± 0.08
T:75MS_1100	45.01 ± 0.77	-1.25 ± 0.02	-1.89 ± 0.03
T:75IG_1000	36.60 ± 0.10	7.41 ± 0.04	5.20 ± 0.03
T:75IG_1100	46.57 ± 0.01	0.65 ± 0.02	0.02 ± 0.01

the thresholds established in the Directive 2003/33/EC [48], which defines the limits for inert (IM) and non-hazardous materials (NHM). All the pigments composed of ES, with high Ni and Cr contents, can be classified as non-hazardous materials as the leached concentrations of Ni and Cr are below the limit of 10 mg/kg. However, an exception was observed with the pigment T:70ES:5Co_1000, which slightly exceeded the Ni limit (13 mg/kg) and hence cannot be considered non-hazardous material. In contrast, the pigment T:70ES:5Co_1100 can be classified as inert material since neither Ni nor Cr were detected in the leachate, and Cu and Zn concentrations did not surpass the limit. The reactivity intensification imparted by the firing temperature improves the immobilization of Cr and Ni [6, 49].

Pigments T:75MS_1100, T:75IG_1000 and T:75IG_1000 can be considered inert since leachates contain low contents

Table 4 Leached concentrations of tested pigments

Pigment ID	As	Cr	Cu	Ni	Pb	Zn
	Leached concentration (mg/kg)[a]					
T:73ES:2Co_1000	-	4.1	-	4.8	-	-
T:73ES:2Co_1100	-	0.7	0.2	0.5	-	0.9
T:70ES:5Co_1000	-	0.8	-	13.0	-	0.3
T:70ES:5Co_1100	-	-	0.8	-	-	1.0
T:75MS_1000	3.1	-	0.1	0.1	-	0.5
T:75MS_1100	-	-	0.1	0.1	-	0.2
T:75IG_1000	-	-	-	-	-	-
T:75IG_1100	-	-	-	-	0.2	-
IM[b]	0.5	0.5	2.0	0.4	0.5	4.0
NHM[b]	2.0	10.0	50.0	10.0	10.0	50.0

[a] mg of leached component per kg of original dry material

[b] Thresholds for inert material (IM) and non-hazardous material (NHM) are defined according to Directive 2003/33/EC [48], for landfilling purposes

of hazardous species, such as As, Cr, Cu, Ni, Pb and Zn. For T:75IG_1100, only a small amount of Pb was detected, which remained below the limit of 0.5 mg/kg [48]. As for the pigment T:75MS_1000, it cannot be categorized as either non-hazardous material or inert material since the leached concentration of As exceeded both the 0.5 and 2 mg/kg limits [48]. However, the pigments T:70ES:5Co_1000 and T:75MS_1000 leached low amounts of Ni and As. In agreement with other studies, these elements can be immobilized in a ceramic matrix, especially when further incorporated in minor amounts, ensuring desirable inertness after the final firing process [10, 12].

Colour Development of Ceramic Paste and Transparent Glaze

As previously mentioned, the colour development of the obtained inorganic pigments was evaluated by adding them to a transparent glaze (G) and to a ceramic paste (P). All the prepared pigments underwent testing in colouring the ceramic paste. The images and CIEL*a*b* colour coordinates are shown in Fig. 4, demonstrating brownish and greyish hues. Furthermore, it is observed that as the amount of incorporated pigment increases from 3 wt% to 5 wt%, the lightness decreases, as well as the red (a*) and yellow (b*) hues of the T: ES: Co_3O_4 pigments fired at 1100 ºC. Similar behaviour was observed for the T: MS_1100 and T: IG_1100 pigments.

As expected, the pigments fired at 1100 ºC showed greater tinting power compared to those fired at 1000 ºC, excepting the pigment T: IG_1100. The pigments with higher colouring power were T:75ES_1100, T:73ES:2Co_1100, T:70ES:5Co_1100 and T: MS_1100, leading to a significant decrease in lightness (> 28%) and the yellow hue compared with paste without pigment; the b* coordinate became positive for T:75ES_1100, T:73ES:2Co_1100, corresponding to a yellow hue, originating brownish ceramic pastes. In contrast, when T:70ES:5Co_1100 and T: MS_ 1100 pigments were added to the ceramic paste, the blue hue increased, leading to greyish ceramic pastes. Based on the colour development of these four pigments in the ceramic paste, their colouration in a transparent glaze was also studied, and data is presented below.

The impact of pigment addition on the sintering process of the ceramic product was assessed by evaluating the total shrinkage and weight loss of the coloured ceramic pastes. The results are presented in Fig. 5. The total shrinkage varied between 4.0 and 12.5%. This variation can be attributed to factors such as the chemical and mineralogical composition of raw materials (including the pigments that contain fluxing elements), mixing ratio, or the particle size distribution [50, 51]. The unpigmented ceramic paste used as a reference showed a total shrinkage of 8%, falling within the typical range of these type of ceramic products (8–13%) [10, 52]. Furthermore, as the pigment addition increased from 3 wt% to 5 wt%, the total shrinkage also increased, except for T:75MS_1100/P5 where the total shrinkage decreased around 45%.

Regarding the weight loss (Fig. 5), the non-pigmented ceramic paste exhibited similar values to the coloured ceramic pastes (5–7 wt%), except for specimen T:75ES_1000/P3, where the value was 14%. This variation can potentially be attributed to the presence of calcium carbonate and calcium sulphate in the T:75ES_1000 pigment, introduced by the electroplating sludge (see Table 2). The sulphate only decomposes above 1000 ºC [8].

Figure 6 shows representative images of coloured transparent glazes fired at 1100 ºC, along with their corresponding CIEL*a*b* colour coordinates. The specimens that presented stronger hues were T:70ES:5Co_1100/G3 and T:73ES:2Co_1100/G3, whose pigments contain cobalt (5 wt% and 2 wt% Co_3O_4, respectively). As anticipated, the

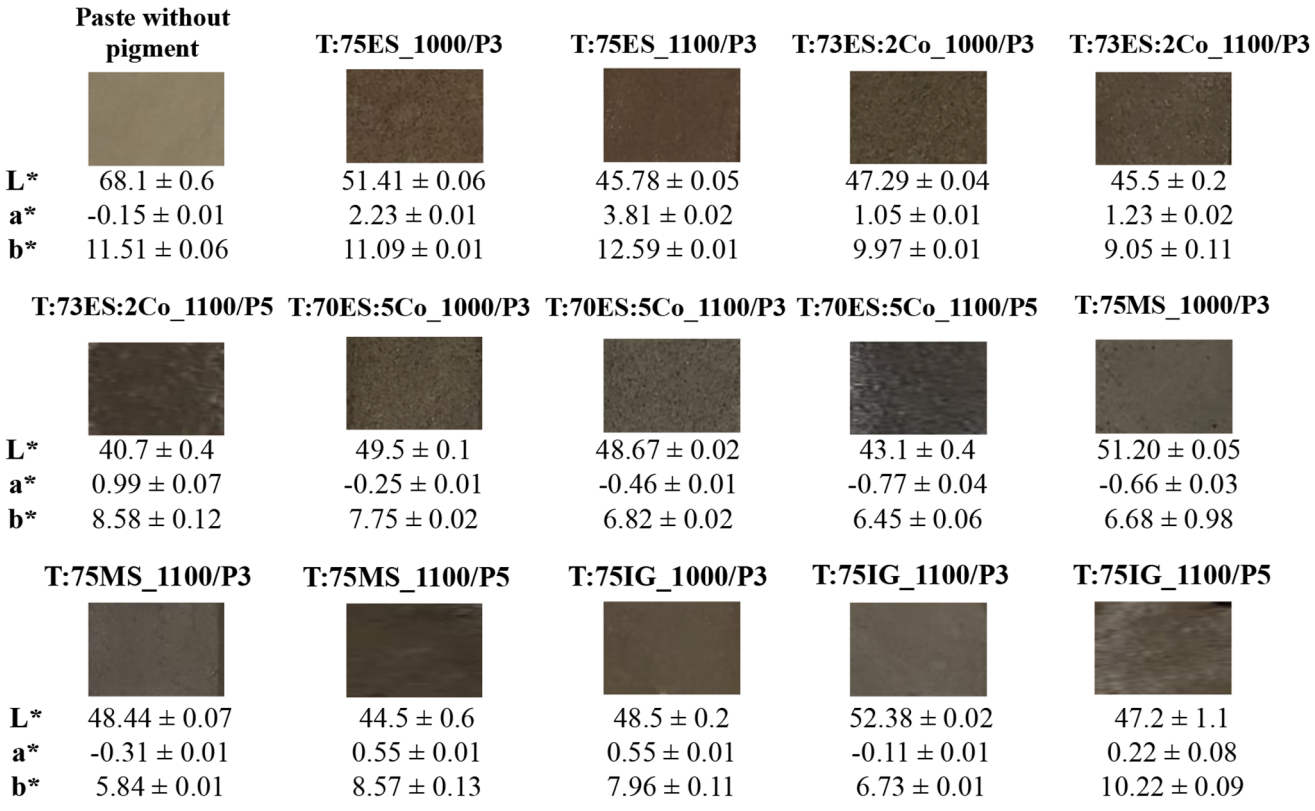

Fig. 4 CIEL*a*b* colour coordinates of ceramic paste specimens loaded with 3–5 wt% of waste-based ceramic pigments and fired at 1220 ºC

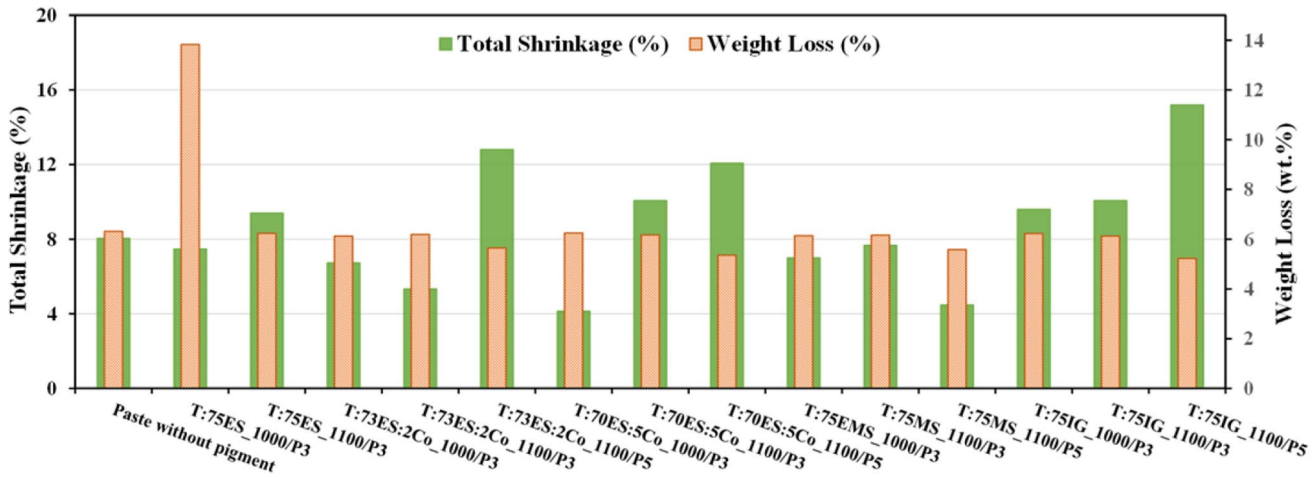

Fig. 5 Effect of the pigment addition on the specimen's total shrinkage and weight loss

glaze lightness decreased with increased cobalt content in the pigment (T:70ES:5Co_1100/G3 > T:73ES:2Co_1100/G3 > T:75ES _1100/G3). In addition, the yellow hue (b*) decreased, while the red and green components (a*) showed no significant variation. Moreover, the specimen T:75ES_1100/G3 demonstrated higher lightness (L* ≈ 51.4) compared to pigments with cobalt, suggesting a weaker colouring power [53]. For this reason, this mixture may not be suitable for colouring this glaze, as it would require a large amount of the pigment to reach the desirable hue [1, 53].

On the other hand, the glaze specimen T: MS_1100/G3 presented a brown hue. As expected, the lightness and yellow hue were high, with a slight green component. The image of T: MS_1100/G3 (Fig. 6) reveals the presence of tiny bubbles, indicating a reaction between the pigment and the transparent glaze. Consequently, this mixture is not suitable for colouring this glaze due to its lack of chemical

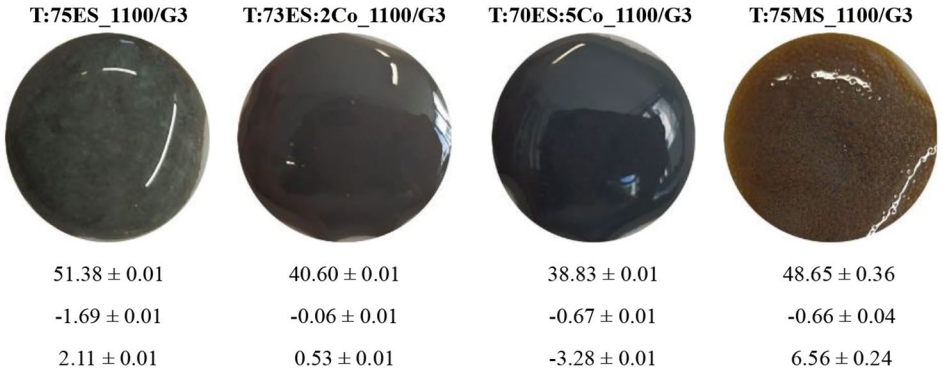

Fig. 6 CIEL*a*b* colour coordinates of transparent glaze specimens loaded with 3 wt% of waste-based ceramic pigments and fired at 1100 ºC

Table 5 Concentration of different elements leached out from the ceramic pastes at room temperature

Specimen ID	Cd	Cr	Fe	Ni	Pb
	Concentration (µg/L)				
	≤20 [(a)]	≤50 [(b)]	≤200 [(b)]	≤20 [(b)]	≤200 [(a)]
Paste without pigment	< 0.4	0	130	6	
T:75ES_1000/P3		0	160	37	
T:75ES_1100/P3		0	53	19	
T:73ES:2Co_1000/P3		5	88	40	
T:73ES:2Co_1100/P3		0	92	18	
T:73ES:2Co_1100/P5		0	62	59	< 0.1
T:70ES:5Co_1000/P3		0	70	31	
T:70ES:5Co_1100/P3		8	110	86	
T:70ES:5Co_1100/P5		0	65	15	
T:75EMS_1000/P3		7	150	9	
T:75MS_1100/P3		0	75	9	
T:75MS_1100/P5		0	55	7	
T:75IG_1000/P3		0	67	6	
T:75IG_1100/P3		4	93	27	
T:75IG_1100/P5		0	82	6	

[(a)] Limit values - drinking water: Council Directive 98/83/EC [54]

[(b)] Limit values - mugs: EU Ceramic Directive 84/500/EEC [28]

stability. According to some authors [1, 2], chemical stability is a crucial requirement for a ceramic pigment.

Acetic acid solution (4% v/v) leaching results of ceramic pastes are shown in Table 5. The limits permitted for Pb and Cd are 200 and 20 µg/L, respectively, in agreement with the European Union Ceramic Directive 84/500/ECC [28]. However, this directive does not specify limits for Cr, Fe and Ni. For this reason, the limits established in the Council Directive 98/83/EC [54] for drinking water were here adopted for these elements, since we are dealing with tableware products. The limit concentrations of Cr, Fe and Ni are 50, 200 and 20 µg/L, respectively.

For all specimens, Cd and Pb concentrations in the leachate did not exceed the permissible limits (200 and 20 µg/L, respectively). Cr and Fe leached concentrations were also below the limits allowed for drinking water (50 and 200 µg/L, respectively). However, for the specimens T:75ES_1000/P3, T:73ES:2Co_1000/P3, T:73ES:2Co_1000/P5, T:70ES:5Co_1000/P3, T:70ES:5Co_1100/P3 and T:75IG_1100/P3, the concentration of Ni in the leachate surpassed the adopted permissible limit (20 µg/L). Thus, the pigments used in these specimens cannot be considered as a substitute for commercial pigments or higher firing temperatures might be used in their preparation. On the other hand, the leached concentration of Ni for the rest of the samples was below the limit. In general, when 3 wt% of pigment is used in the ceramic paste, the concentration of toxic species in the leachate was lower than the limit values for Cd, Cr, Fe, Ni and Pb. Consequently, the T:75ES_1100, T:73ES:2Co_1100, T:75MS_1000, T:75MS_1100 and T:75IG_1000 pigments can be used to colouring the ceramic paste, replacing partially or entirely the commercial pigments, depending on the desired colour. Vilarinho et al. [55] performed a life cycle assessment (LCA) on a stoneware cups production and the use of pigment represented 15% of the total carbon footprint of the process. Further, according to Alifieris et al. [56] very little information on this subject can be found in the literature. However, through a LCA on a Cr-based pigment, the authors concluded that the major impact, 96% of the total CO_2 emissions, are related to the raw materials. Therefore, the use of wastes as raw materials for pigment production is very appealing once it can reduce: (i) the total CO_2 emissions of the production process, (ii) the quantity of wastes deposited in landfills; (iii) the dangerous potential of certain species, since they are immobilized in the pigment structure or in the final products; (iv) the consumption of virgin raw materials. Further, as the used wastes still do not have a commercial value in many countries, their price can be a commercial advantage for the pigment industry.

Conclusions

This work aimed to produce inorganic pigments from four industrial wastes (tionite, electroplating sludge, mill scale and iron grit) and assess their colouring potential in a ceramic paste and in a transparent glaze. The obtained results showed that:

- Dark pigments were produced with the mixtures T: ES: Co_3O_4, T: MS and T: IG, independently of the firing temperature (1000ºC and 1100 ºC).
- Leaching tests revealed that the developed pigments can be considered non-hazardous or inert, since their leachates exhibited low concentrations of toxic species, except for T:70ES:5Co_1000 and T:75MS_1000 pigments that leached Ni and As, respectively, in concentrations slightly above the limit (Ni:13.0 mg/kg and As:3.1 mg/kg).
- The increase in firing temperature improved the immobilization of toxic species.
- The pigments fired at 1100ºC presented higher tinting power than those fired at 1000ºC. T:75ES_1100, T:73ES:2Co_1100, T:70ES:5Co_1100 and T: MS_ 1100 showed stronger colouring power, resulting in appealing brownish and greyish hues in both products.
- Leaching results attest the safety of using T:75ES_1100, T:73ES:2Co_1100, T:75MS_1000, T:75MS_1100 and T:75IG_1000 pigments in ceramic stoneware paste. Therefore, partial or complete replacement of commercial pigments is feasible.

Concluding, this work provided a new value-added application for the selected hazardous industrial wastes as pigments for use in ceramic products. By effectively removing hazardous wastes from the environment and reducing the dependency on primary raw materials, this approach demonstrates significant potential for developing sustainable and eco-friendly products.

Acknowledgements The authors gratefully acknowledge Huelva University for providing the waste and the collaboration with the Department of Materials Engineering of the University of Aveiro, Portugal. João Carvalheiras (SFRH/BD/144562/2019) wish to thank Fundação para a Ciência e Tecnologia (FCT) for supporting their work.

Author Contributions Conceptualization, D.C.P.-G., I.S.V., S.M.P.-M., J.C., M.P.S., J.P.B. and J.A.L.; Data curation, D.C.P.-G., I.S.V. and J.C.; Formal analysis, D.C.P.-G., I.S.V., J.C., M.P.S., J.P.B. and J.A.L.; Funding acquisition, J.P.B. and J.A.L.; Investigation, D.C.P.-G., I.S.V., J.C. and J.A.L.; Methodology, D.C.P.-G., I.S.V., J.C. and M.P.S.; Project administration, J.P.B. and J.A.L.; Resources, M.P.S. and J.P.B.; Supervision, I.S.V., S.M.P.-M., M.P.S., J.P.B. and J.A.L.; Validation, D.C.P.-G., I.S.V. and J.C.; Visualization, M.P.S., J.P.B. and J.A.L.; Writing—original draft, D.C.P.-G. and I.S.V.; Writing—review & editing, J.C, S.M.P.-M., M.P.S., J.P.B. and J.A.L. All authors have read and agreed to the published version of the manuscript.

Funding This work was developed within the scope of the project CICECO-Aveiro Institute of Materials, UIDB/50011/2020, UIDP/50011/2020 & LA/P/0006/2020, financed by national funds through the FCT/MCTES (PIDDAC) and it has been also funded by the project ENFRIMA (UHU-202020).
Open access funding provided by FCT|FCCN (b-on).

Data Availability Not applicable.

Declarations

Conflict of interest The authors declare no conflict of interest.

References

1. Monros, G.: Pigment, Ceramic. Encyclopedia of Color Science and Technology 1–15. (2013). https://doi.org/10.1007/978-3-642-27851-8_181-3
2. Hempelmann, U., Buxbaum, G., Völz, H.G.: Introduction. In: Buxbaum G, Pfaff AG (eds) In Industrial Inorganic Pigments (2005)
3. Singh, H.B., Bharati, K.A.: Handbook of Natural Dyes and Pigments (2014)
4. Rutherford, J., Stout, G.L.: Painting materials: A short encyclopedia (Gettens. J. Chem. Educ. **19** (1942). https://doi.org/10.1021/ed019p500.2
5. Carneiro, J., Tobaldi, D.M., Capela, M.N., et al.: Synthesis of ceramic pigments from industrial wastes: Red mud and electroplating sludge. Waste Manage. **80**, 371–378 (2018). https://doi.org/10.1016/j.wasman.2018.09.032
6. Matovic, L., Vujasin, R., Kumric, K., et al.: Designing of technological scheme for conversion of Cr-rich electroplating sludge into the black ceramic pigments of consistent composition, following the principles of circular economy. J. Environ. Chem. Eng. **9** (2021). https://doi.org/10.1016/j.jece.2021.105038
7. Hajjaji, W., Costa, G., Zanelli, C., et al.: An overview of using solid wastes for pigment industry. J. Eur. Ceram. Soc. **32**, 753–764 (2012). https://doi.org/10.1016/j.jeurceramsoc.2011.10.018
8. European Commission: Closing the loop - An EU action plan for the Circular Economy. Brussel (2015)
9. Carneiro, J., Tobaldi, D.M., Hajjaji, W., et al.: Red mud as a substitute coloring agent for the hematite pigment. Ceram. Int. **44**, 4211–4219 (2018). https://doi.org/10.1016/j.ceramint.2017.11.225
10. Vilarinho, I.S., Carneiro, J., Pinto, C., et al.: Development of coloured stoneware bodies through the incorporation of industrial Cr/Ni electroplating sludge. Sustain. (Switzerland). **13**, 1–13 (2021). https://doi.org/10.3390/su13041999
11. Hajjaji, W., Pullar, R.C., Zanelli, C., et al.: Compositional and chromatic properties of strontium hexaferrite as pigment for

ceramic bodies and alternative synthesis from wiredrawing sludge. Dyes Pigm. **96**, 659–664 (2013). https://doi.org/10.1016/j.dyepig.2012.10.011
12. Vilarinho, I.S., Lopes, A.L., Carneiro, J., et al.: A new added-value application for steel wire drawing mill scale waste in stoneware ceramic products. Met. (Basel). **11**, 1–13 (2021). https://doi.org/10.3390/met11040661
13. Prim, S.R., Folgueras, M.V., de Lima, M.A., Hotza, D.: Synthesis and characterization of hematite pigment obtained from a steel waste industry. J. Hazard. Mater. **192**, 1307–1313 (2011). https://doi.org/10.1016/j.jhazmat.2011.06.034
14. Bautista-Marín, J.D., Esguerra-Arce, A., Esguerra-Arce, J.: Use of an industrial solid waste as a pigment in clay bricks and its effects on the mechanical properties. Constr. Build. Mater. **306**, 124848 (2021). https://doi.org/10.1016/j.conbuildmat.2021.124848
15. Pereira, O.C., Bernardin, A.M.: Ceramic colorant from untreated iron ore residue. J. Hazard. Mater. **233–234**, 103–111 (2012). https://doi.org/10.1016/j.jhazmat.2012.06.057
16. Hajjaji, W., Seabra, M.P., Labrincha, J.A.: Evaluation of metal-ions containing sludges in the preparation of black inorganic pigments. J. Hazard. Mater. **185**, 619–625 (2011). https://doi.org/10.1016/j.jhazmat.2010.09.063
17. Contreras, M., Martín, M.I., Gázquez, M.J., et al.: Valorisation of ilmenite mud waste in the manufacture of commercial ceramic. Constr. Build. Mater. **72**, 31–40 (2014). https://doi.org/10.1016/j.conbuildmat.2014.08.091
18. Pérez-Moreno, S.M., Gázquez, M.J., Barneto, A.G., Bolívar, J.P.: Thermal characterization of new fire-insulating materials from industrial inorganic TiO2 wastes. Thermochim Acta. **552**, 114–122 (2013). https://doi.org/10.1016/j.tca.2012.10.021
19. Vilarinho, I.S., Lopes, A.L., Carneiro, J., et al.: A new added-value application for steel wire drawing mill scale waste in stoneware ceramic products. Met. (Basel). **11** (2021). https://doi.org/10.3390/met11040661
20. Legodi, M.A., de Waal, D.: The preparation of magnetite, goethite, hematite and maghemite of pigment quality from mill scale iron waste. Dyes Pigm. **74**, 161–168 (2007). https://doi.org/10.1016/j.dyepig.2006.01.038
21. Magalhães, J.M., Silva, J.E., Castro, F.P., Labrincha, J.A.: Kinetic study of the immobilization of galvanic sludge in clay-based matrix. J. Hazard. Mater. **121**, 69–78 (2005). https://doi.org/10.1016/j.jhazmat.2005.01.022
22. Vilarinho, I.S., Filippi, E., Seabra, M.P.: Development of eco-ceramic wall tiles with bio-CaCO3 from eggshells waste. Open. Ceram. **9**, 100220 (2022). https://doi.org/10.1016/j.oceram.2022.100220
23. Cavalcante, P.M.T., Dondi, M., Guarini, G., et al.: Colour performance of ceramic nano-pigments. Dyes Pigm. **80**, 226–232 (2009). https://doi.org/10.1016/j.dyepig.2008.07.004
24. Yuan, R., Guo, M., Li, C., et al.: Detection of early bruises in jujubes based on reflectance, absorbance and Kubelka-Munk spectral data. Postharvest Biol. Technol. **185**, 111810 (2022). https://doi.org/10.1016/j.postharvbio.2021.111810
25. Commission Internationale d'Eclairage (CIE): Recommendations on Uniform Color spaces, Color-Difference equations, and Metric Color terms. Color. Res. Appl. **2**, 5–6 (1977). https://doi.org/10.1002/j.1520-6378.1977.tb00102.x
26. Schanda, J.: Colorimetry: Understanding the CIE System. Wiley (2007)
27. CEN: European Committee for Standardization: EN 12457-2 Leaching - Compliance test for leaching of granular waste materials and sludges — Part 2: One stage batch test at a liquid to solid ratio of 10 l/kg for materials with particle size below 4 mm ((2002). without or with size reduction)
28. Council of the European Union: Council Directive 84/500/EEC of 15 October 1984 on the approximation of the laws of the Member States relating to ceramic articles intended to come into contact with foodstuffs. Official J. Eur. Communities 26–30 (1984)
29. Gorai, B., Jana, R.K., Premchand: Characteristics and utilisation of copper slag - A review. Resour. Conserv. Recycl. **39**, 299–313 (2003). https://doi.org/10.1016/S0921-3449(02)00171-4
30. Guo, Z., Zhu, D., Pan, J., et al.: Improving beneficiation of copper and iron from copper slag by modifying the molten copper slag. Met. (Basel). **6** (2016). https://doi.org/10.3390/met6040086
31. Gabasiane, T.S., Danha, G., Mamvura, T.A., et al.: Characterization of copper slag for beneficiation of iron and copper. Heliyon. **7**, e06757 (2021). https://doi.org/10.1016/j.heliyon.2021.e06757
32. Carneiro, J., Tobaldi, D.M., Capela, M.N., et al.: Waste-based pigments for application in ceramic glazes and stoneware bodies. Materials. **12** (2019). https://doi.org/10.3390/ma12203396
33. Buxbaum, G., Pfaff, G.: Industrial Inorganic Pigments. Wiley (2005)
34. Teller, R.G., Antonio, M.R., Grau, A.E., et al.: The chemistry of the thermal decomposition of pseudobrookite ferrous titanium oxides. J. Solid State Chem. **88**, 351–367 (1990). https://doi.org/10.1016/0022-4596(90)90230-U
35. Riyas, S., Yasir, V.A., Mohan Das, P.N.: Crystal structure transformation of TiO2 in presence of Fe2O3 and NiO in air atmosphere. Bull. Mater. Sci. **25**, 267–273 (2002). https://doi.org/10.1007/BF02704118
36. Lin, K.N., Wu, S.K.: Oxidation behavior of Ti 50Ni 40Cu 10 shape-memory alloy in 700-1,000 °c air. Oxid. Met. **71**, 187–200 (2009). https://doi.org/10.1007/s11085-008-9135-9
37. Xirouchakis, D., Fritsch, S., Putnam, R.L., et al.: Thermochemistry and the enthalpy of formation of synthetic end-member (CaTiSiO5) titanite. Am. Mineral. **82**, 754–759 (1997). https://doi.org/10.2138/am-1997-7-813
38. Ullrich, A., Rölle, N., Horn, S.: From wustite to hematite: Thermal transformation of differently sized iron oxide nanoparticles in air. J. Nanopart. Res. **21**, 1–8 (2019). https://doi.org/10.1007/s11051-019-4607-1
39. Monazam, E.R., Breault, R.W., Siriwardane, R.: Kinetics of magnetite (Fe3O4) oxidation to hematite (Fe2O3) in air for chemical looping combustion. Ind. Eng. Chem. Res. **53**, 13320–13328 (2014). https://doi.org/10.1021/ie501536s
40. Gyurov, S., Rabadjieva, D., Kovacheva, D., Kostova, Y.: Kinetics of copper slag oxidation under nonisothermal conditions. J. Therm. Anal. Calorim. **116**, 945–953 (2014). https://doi.org/10.1007/s10973-013-3569-2
41. Chen, J.H., Mi, W.J., Chen, H.Y., et al.: Iron oxide recovery from fayalite in water vapor at high temperature. J. Min. Metall.Sect. B. **54**, 1–8 (2018). https://doi.org/10.2298/JMMB160926011C
42. Gennari, F.C., Pasquevich, D.M.: Kinetics of the anatase–rutile transformation in TiO2 in the presence of Fe2O3. J. Mater. Sci. **33**, 1571–1578 (1998)
43. Matteucci, F., Cruciani, G., Dondi, M., et al.: Crystal structure, optical properties and colouring performance of karrooite MgTi2O5 ceramic pigments. J. Solid State Chem. **180**, 3196–3210 (2007). https://doi.org/10.1016/j.jssc.2007.08.029
44. Han, A.J., Ye, M.Q., Zhang, Z.M., et al.: Crystal structure and Optical properties of CoCr2O4–NiCr2O4 solid solutions prepared by low-temperature Combustion Synthesis Method. Adv. Mat. Res. **616–618**, 1877–1881 (2013). https://doi.org/10.4028/www.scientific.net/AMR.616-618.1877
45. Gayo, G.X.: Fabricación De Pigmentos cerámico con criterios Sustentables. Universitat Jaume I (2017)
46. Dondi, M., Matteucci, F., Cruciani, G., et al.: Pseudobrookite ceramic pigments: Crystal structural, optical and technological properties. Solid State Sci. **9**, 362–369 (2007). https://doi.org/10.1016/j.solidstatesciences.2007.03.001
47. Carneiro, J., Capela, M.N., Tobaldi, D.M., et al.: Red mud and electroplating sludge as coloring agents of distinct glazes: The

influence of heat treatment. Mater. Lett. **223**, 166–169 (2018). https://doi.org/10.1016/j.matlet.2018.04.013
48. Council of the European Union: Directive 2003/33/EC of 19 December 2002 establishing criteria and procedures for the acceptance of waste at landfills pursuant to article 16 of and annex II to Directive 1999/31/EC. Official J. Eur. Communities. **11**, 27–49 (2003)
49. Yin, X., Huang, J., Pu, Z., et al.: Effect of the calcination temperature on the cation distribution and optical properties of Mg0.5Co0.5CrAlO4 spinel pigment. Ceram. Int. **47**, 17167–17176 (2021). https://doi.org/10.1016/j.ceramint.2021.03.027
50. Salem, A., Jazayeri, S.H., Rastelli, E., Timellini, G.: Dilatometeric study of shrinkage during sintering process for porcelain stoneware body in presence of nepheline syenite. J. Mater. Process. Technol. **209**, 1240–1246 (2009). https://doi.org/10.1016/j.jmatprotec.2008.03.033
51. Das, S.K., Dana, K., Singh, N., Sarkar, R.: Shrinkage and strength behaviour of quartzitic and kaolinitic clays in wall tile compositions. Appl. Clay Sci. **29**, 137–143 (2005). https://doi.org/10.1016/j.clay.2004.10.002
52. Sooksaen, P., Karawatthanaworrakul, S.: The properties of Southern Thailand clay-based porous ceramics fabricated from different pore size templates. Appl. Clay Sci. **104**, 295–302 (2015). https://doi.org/10.1016/j.clay.2014.12.009
53. Völz, H.G., Kischkewitz, J., Woditsch, P., et al.: Pigments, Inorganic. In: Ullmann's Encyclopedia of Industrial Chemistry. Wiley-VCH Verlag GmbH & Co. KGaA, Weinheim, Germany (2000)
54. Council of the European Union: Council Directive 98/83/EC of 3 November 1998 on the quality of water intended for human consumption. Official J. Eur. Communities 1–15 (1998)
55. Vilarinho, I.S., Dias, A.C., Carneiro, J., et al.: Red mud valorization in stoneware pastes: Technical and environmental assessment. Sustainable Mater. Technol. **38**, e00762 (2023). https://doi.org/10.1016/j.susmat.2023.e00762
56. Alifieris, O., Katsourinis, D., Giannopoulos, D., Founti, M.: Process simulation and life cycle assessment of ceramic pigment production: A case study of green cr2o3. Processes. **9** (2021). https://doi.org/10.3390/pr9101731